ChemPubSoc Europe
DOI: 10.1002/chem.201802317
CHEMISTRY
A European Journal
Communication

Thin Films

Obtaining a Low and Wide Atomic Layer Deposition Window (150–275 °C) for In_2O_3 Films Using an In^{III} Amidinate and H_2O

Sang Bok Kim,[a] Ashwin Jayaraman,[a] Danny Chua,[a] Luke M. Davis,[a] Shao-Liang Zheng,[a] Xizhu Zhao,[a] Sunghwan Lee,[b] and Roy G. Gordon*[a]

Abstract: Indium oxide is a major component of many technologically important thin films, most notably the transparent conductor indium tin oxide (ITO). Despite being pyrophoric, homoleptic indium(III) alkyls do not allow atomic layer deposition (ALD) of In_2O_3 using water as a co-precursor at substrate temperatures below 200 °C. Several alternative indium sources have been developed, but none allows ALD at lower temperatures except in the presence of oxidants such as O_2 or O_3, which are not compatible with some substrates or alloying processes. We have synthesized a new indium precursor, tris(*N*,*N'*-diisopropylformamidinato)indium(III), compound **1**, which allows ALD of pure, carbon-free In_2O_3 films using H_2O as the only co-reactant, on substrates in the temperature range 150–275 °C. In contrast, replacing just the H of the anionic *i*PrNC(H)N*i*Pr ligand with a methyl group (affording the known tris(*N*,*N'*-diisopropylacetamidinato)indium(III), compound **2**) results in a considerably higher and narrower ALD window in the analogous reaction with H_2O (225–300 °C). Kinetic studies demonstrate that a higher rate of surface reactions in both parts of the ALD cycle gives rise to this difference in the ALD windows.

Thin films containing indium, especially multi-component alloys,[1] have enormous technological significance. In thin-film photovoltaics, mixed oxide-sulfides of indium act as electron-transport layers,[1c,d] and copper-indium-gallium-sulfide (CIGS) serves as an absorber layer.[1c,d] By far the most common use is in indium tin oxide (ITO), a transparent conducting oxide (TCO)[2] widely used in flat-panel and touch-sensitive displays as well as thin-film solar cells.[3] ITO films are often deposited by magnetron sputtering[2b,4] or chemical vapor deposition (CVD).[5] Though these methods provide high growth rates on planar substrates, high deposition temperatures, thickness variation, and sputtering damage can be issues when applied to very thin films or non-flat substrates.[4–6]

Due to increasing demand for highly conformal, very thin films (e.g., electron transport layers can sometimes be as thin as 10–20 nm) containing indium as part of a multi-component composition, it would be advantageous to grow In_2O_3 thin films by atomic layer deposition (ALD).[6b,7] In order to allow alloying, it would be especially helpful to find a broad range of slightly elevated temperatures in which the growth rate is constant and the film deposition proceeds by canonical alternating cycles of surface saturation, that is, a low and wide ALD window.[6b,7] A low ALD temperature is important for sensitive substrates such as polymers, organic light absorbers, and those inorganic multi-layered devices having the possibility of interlayer contamination by thermally activated diffusion. A wide ALD window would allow for the doping of In^{III} into a broader range of alloyed materials, whether those are other metal oxides or indium chalcogenides.[1d,6b,7] However, low-temperature ALD of In_2O_3 has remained a persistent challenge.[1d,6a,8] The only reports of ALD of In_2O_3 below 200 °C require an oxidant, either O_2 or O_3 (Figure 1, Table S1 in the Supporting

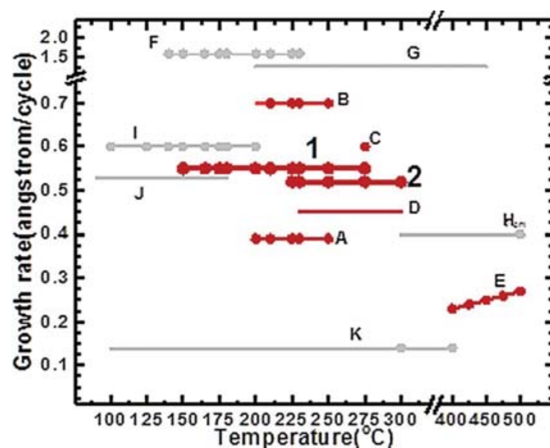

Figure 1. Growth rate versus temperature for all In_2O_3 ALD processes. Lines represent the carbon-free ALD window, and circles denote temperatures at which the film resistivity was reported to be $< 10^{-2}$ Ω·cm. Red markers indicate H_2O as the sole oxygen source; gray markers indicate another oxygen source such as O_3, H_2O_2, or O_2. The indium sources are **1** and **2**[14a] (this work), TMIn (A[8g]), $Et_2In[N(SiMe_3)_2]$ (B[8a]), DADI (C[8j]), $In[C(N\textit{i}Pr_2)(N\textit{i}Pr)_2]_3$ (D[8h]), $InCl_3$ (E[8d,e]), InCp (F,[6a] G[8b]), TEIn (I[8f]), $Me_2In(EDPA)$ (J[8k]), and $In(tmhd)_3$ (K[8c]).

[a] Dr. S. B. Kim, Dr. A. Jayaraman, D. Chua, Dr. L. M. Davis, Dr. S.-L. Zheng, Dr. X. Zhao, Prof. Dr. R. G. Gordon
Department of Chemistry and Chemical Biology
Harvard University
12 Oxford Street, Cambridge, MA 02138 (USA)
E-mail: gordon@chemistry.harvard.edu

[b] Prof. Dr. S. Lee
Department of Mechanical Engineering
Baylor University
One Bear Place #97536, Waco, TX 76798-7356 (USA)

Supporting information and the ORCID identification numbers for the authors of this article can be found under: https://doi.org/10.1002/chem.201802317.

© 2018 Wiley-VCH Verlag GmbH & Co. KGaA, Weinheim

Information). The use of an oxygen source other than water limits the compatibility of the process for alloying or depositing on some substrates in multi-layered devices by oxidizing other low-valent metal oxides (e.g., Cu^{I}_2O,[9] $W^{III}_2O_3$,[10] or $Sn^{II}O$[11]), and is likely to be a reason for non-uniform films.[6a,8b]

The lack of a water-based low-temperature ALD process for In_2O_3 seems especially striking when one considers that its aluminum congener, Al_2O_3, provides the canonical example of an ALD process operating at temperatures as low as 33 °C using alternating doses of water and trimethylaluminum(III) (TMA).[12] However, trimethylindium(III) (TMIn) affords ALD In_2O_3 with water only above 200 °C.[8g] Mixed alkyl/amido compounds such as $Et_2In[N(SiMe_3)_2]$ offer enhanced growth rates, but retain carbon in the films below 200 °C.[8a] Interestingly, the higher growth rate (≈0.7 Å/cycle) for $Et_2In[N(SiMe_3)_2]$ than TMIn (≈0.39 Å/cycle) appears to indicate a higher reactivity of water with indium–nitrogen bonds than indium–carbon bonds. The lower growth rate using TMIn may reflect a lower reactivity of water to chemisorbed TMIn or of TMIn to chemisorbed water.

Herein, we report a new In^{III} precursor, tris(*N*,*N′*-diisopropylformamidinato)indium(III) (**1**, Scheme 1), and a study of its reactivity for ALD of In_2O_3. We have selected this particular amidinate ligand in light of the excellent volatility and reactivity of its Ca^{II} complex.[13] Compound **1** enables ALD of In_2O_3 films in the temperature range 150–275 °C, using water as the oxygen source, at a constant growth rate of 0.55 Å/cycle. All films deposited in the ALD window show resistivity ($1–4\times10^{-3}$ Ω·cm) and visible-light transmittance (≥80%) suitable for a TCO. In general a TCO[2b] should possess a resistivity on the order of 10^{-3} Ω·cm or less, and transmittance above 80%.

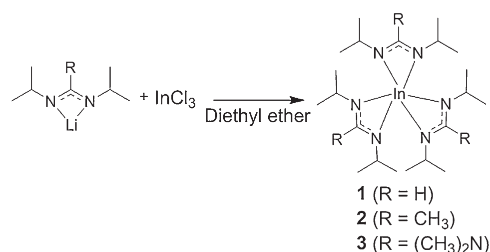

Scheme 1. Synthesis of In^{III} amidinates (**1**, **2**) and In^{III} guanidinate (**3**).

We note four special features of these results. First, only water is used as an oxygen source for this low-temperature ALD. Second, the In^{III} compound **1** is neither oxygen-sensitive, like commercially available $In^{I}Cp$,[6a,8b] nor pyrophoric, like In^{III} alkyls. Third, among all In_2O_3 ALD reactions with water as the oxygen source, **1** allows both the lowest ALD onset temperature and the widest ALD window (Figure 1 and Table S1). A great number of ALD windows of metal oxides overlap with that of ALD using **1** and H_2O, enabling ALD of multicomponent films.[7] Fourth, comparison of the ALD window and kinetics studies of the formamidinate **1** with its acetamidinate congener **2**[14] (Scheme 1) highlights the extraordinary reactivity of **1**. It was observed that a surface saturated with chemisorbed **1** completes the surface reactions with H_2O 3–4 times faster than a surface saturated with chemisorbed **2** at 250 °C. This higher rate of surface reactions is believed to generate the low and wide ALD window. The enhanced reactivity of compounds bearing *N*,*N′*-diisopropylformamidinato ligands is expected to be widely useful in developing precursors for ALD at low temperatures.

Single crystals of colorless **1** were grown by sublimation and the solid-state structure determined by X-ray crystallography (Figure 2, Tables S2 and S3 in the Supporting Information). The pseudo-octahedral molecule has a chiral, propeller shape, as expected for a homoleptic tris(amidinate),[15] and the enantiomers crystallize together in the centrosymmetric space group $P2_1/n$. Every atom of the molecule is disordered over four positions. Nonetheless, the structure is generally unremarkable, with an average In–N distance, 2.252(13) Å, which is not significantly different from the 2.254(3)–2.271(3) Å found in two In^{III} guanidinates or the 2.233(5)–2.238(6) Å found in **2**.[8h,14b]

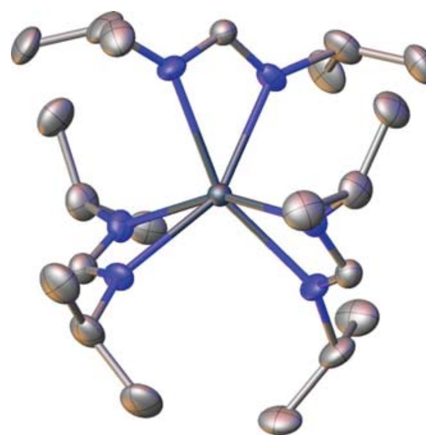

Figure 2. Solid-state structure of **1** determined by X-ray diffraction. Hydrogen atoms are omitted and only one disorder component is shown for clarity. In–N distances, clockwise from top left (Å): 2.292(13), 2.284(12), 2.218(13), 2.233(13), 2.223(13), 2.262(12).

To compare the thermal stability and volatility of **1** with those of **2** and commercially available $In(acac)_3$, thermogravimetric analysis (TGA) experiments were performed for all three compounds. Figure 3a shows that both **1** and **2** evaporate completely in a single step without leaving residues from thermal decomposition. By utilizing a faster heating rate and larger amount of compound, the complete evaporation of **1** and **2** can be shifted to higher temperature, demonstrating thermal stability on the TGA timescale up to at least 320 °C for **1** and 370 °C for **2** (Figure 3a and Figure S4a,b). In the log–log plot of Figure 3b, the evaporation rates of both **1** and **2** increase linearly with temperature, confirming a single mass-loss mechanism (evaporation). The evaporation rate of **1** is clearly higher than those of both **2** and $In(acac)_3$. From Figure 3b, we can estimate the heating temperatures necessary to afford the same evaporation rate. For instance, to obtain an evaporation rate of 0.1 $mg\,min^{-1}\,cm^{-2}$, **1** requires heating to ca. 127 °C, whereas **2** must be heated ca. 40 °C higher and $In(acac)_3$ about another 25 °C higher.

© 2018 Wiley-VCH Verlag GmbH & Co. KGaA, Weinheim

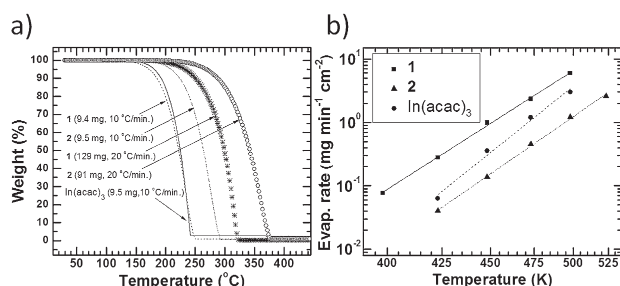

Figure 3. a) Ramp TGA curves of **1** (dashed line, 9.4 mg, 10 °C min^{-1}); **2** (dash dot dotted line, 9.5 mg, 10 °C min^{-1}); In(acac)$_3$ (solid line, 9.3 mg, 10 °C min^{-1}); **1** (star, 129 mg, 20 °C min^{-1}); **2** (open circle, 91 mg, 20 °C min^{-1}). b) Plot of evaporation rate (mg min^{-1} cm^{-2}, log scale) versus inverse temperature (K, log scale): **1** (closed square, solid line); **2** (closed triangle, dash dot dotted line); In(acac)$_3$ (closed circle, dashed line).

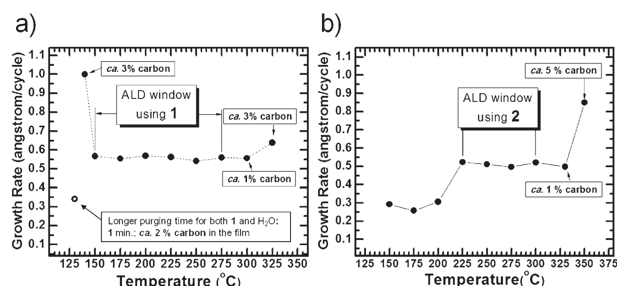

Figure 4. a) ALD windows using H_2O and a) **1**, and b) **2**. These ALD recipes are described in the Supporting Information.

Figure 4 shows the temperature window of In_2O_3 ALD combining water and **1** (Figure 4a, 150–275 °C, 0.55 Å/cycle) or **2** (Figure 4b, 225–300 °C, 0.52 Å/cycle). The precursor reservoir was heated to 125 °C to vaporise **1** and to 140 °C for **2**. Although **2** should be heated to ca. 165 °C to equalize the vaporisation rate with **1**, our ALD valves constrain this temperature to 140 °C; instead, we used two doses of **2** to saturate the surface (Figure S1, Supporting Information). Films at the upper end of the ALD windows of **1** and **2** contain ca. 1 at.% carbon (Figure S7). Thermal decomposition of the precursor or its by-products on the growth surface is common at the upper end of ALD windows.

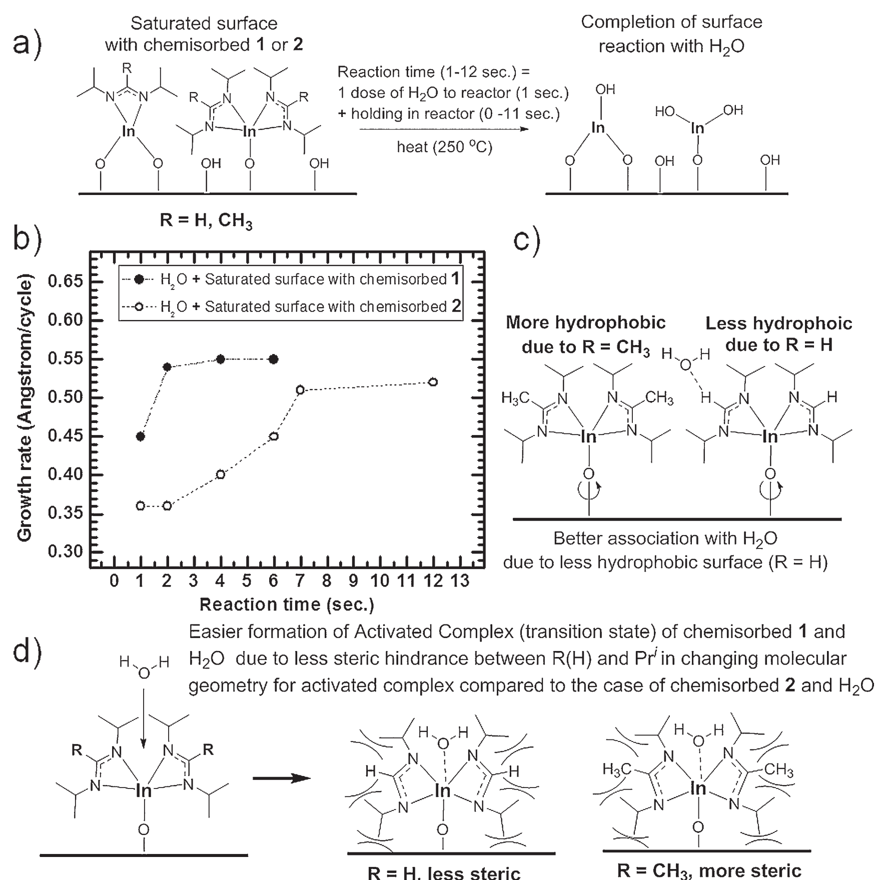

Figure 5. Kinetic study on In_2O_3 ALD using **1** versus **2**, a) plausible mechanism of surface reaction between saturated surface with chemisorbed **1** or **2** and H_2O, b) growth rate (at 250 °C) versus reaction time of H_2O and surface saturated with chemisorbed **1** (closed circle, dash dotted line) or **2** (open circle, dashed line), c) difference between chemisorbed **1** and **2** in hydrophilicity, d) formation of activated complex of chemisorbed **1** or **2** and H_2O with resulting steric hindrances.

© 2018 Wiley-VCH Verlag GmbH & Co. KGaA, Weinheim

In order to understand why the lowest ALD temperature using **1** is so much lower than that using **2**, kinetic studies were performed at a surface temperature of 250 °C (selected because it falls neatly within both ALD windows). To compare the reactivity of the two precursors, in parallel experiments we saturated the growth surface with **1** or **2**, and then determined the exposure time necessary for water to saturate the surface. Utilizing the reaction between the saturated surface and H_2O vapor allows us to avoid confounding the reaction rate with the difference in dosing time and vapor pressure between **1** and **2** at 250 °C. Interestingly, the high similarity of the ALD growth rates also allows us to rule out confounds that would result from different extents of surface coverage-in order to obtain growth rates of 0.55 and 0.52 Å/cycle, the coverage of **1**-saturated and **2**-saturated surfaces must be comparable. The results of these experiments are shown in Figure 5, where reaction time is defined as the sum of the dosing time of H_2O (1 s, meaning the ALD valve for H_2O is opened to the reaction chamber for 1 s) and the time H_2O is held in the reaction chamber before purging begins. The reaction of H_2O with the surface saturated by **1** (2 s to achieve the ALD growth rate) is completed much more quickly than the reaction with the surface saturated by **2** (7 s to obtain the ALD growth rate). The observation that water reacts more readily with **1**-saturated surfaces than **2**-saturated surfaces at the same temperature helps to rationalize the lower ALD growth onset temperature for **1** than for **2**. The surface reactions are able to proceed to completion more easily for **1** than for **2**, and consequently lower growth temperatures are available.

Because the ALD reactions take place on surfaces at elevated temperatures, it is difficult to determine a detailed mechanism giving rise to this enhanced reactivity of **1**. Without direct evidence, we are unable to adjudicate between several alternative explanations of the enhanced reactivity of **1**, including steric effects (Figure 5 d); hydrophilicity arguments, wherein a more hydrophilic **1**-saturated surface allows better association with H_2O (Figure 5 c); and the possibility that the surface reaction of chemisorbed **1** with H_2O affords In–OH and organic byproducts by a different mechanism (e.g., hydrolysis of formamidinate[16]) from the simple acid-base reaction to afford In–OH and amidine (expected for chemisorbed **2**).

Figure 6 shows an SEM image and XRD pattern for the In_2O_3 ALD film. Further SEM images (Figures S8 and S9) and XRD patterns (Figures S5 and S6) of the In_2O_3 ALD films grown in this study are provided in the Supporting Information. Hall-effect measurements afford the Hall mobility, carrier concentration, and resistivity for these films (Figures S14 and S15). The resistivity of all films grown in the ALD windows of **1** and **2** were found to be in the range $1–4\times10^{-3}$ Ω·cm which is sufficiently low for use as a TCO (Figure S14). UV/Vis experiments for these films demonstrate the high transmittance in the visible range (>80 %, Figures S10–S12).

In summary, a new indium(III) compound, **1**, was prepared and its utility for ALD of In_2O_3 was demonstrated. Of the In_2O_3 ALD processes using H_2O as the co-reactant, ALD using **1** showed the lowest and widest ALD window (150–275 °C). This low ALD temperature is believed to result from the high rate of the surface reaction of chemisorbed **1** with H_2O, as well as of **1** with surface hydroxyl groups. In addition to extending the ALD window to enhance the compatibility of In_2O_3 ALD with other metal oxides and indium chalcogenides, the higher reactivity reduces the overall time required to deposit a film of a given thickness. Strikingly, all films grown in the ALD window of **1** have a low resistivity ($\approx10^{-3}$ Ω·cm) suitable for a TCO.

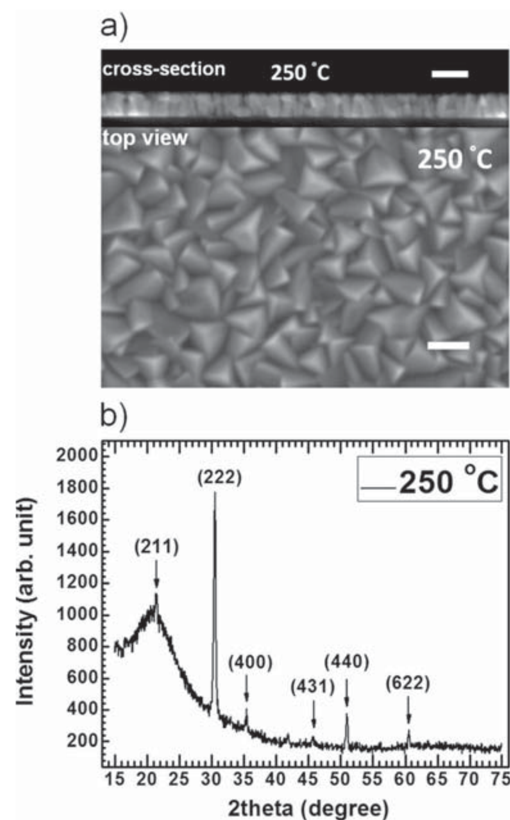

Figure 6. In_2O_3 ALD films grown with **1** and H_2O at 250 °C; a) SEM image (scale bar: 100 nm) of an In_2O_3 film (thickness: 72 nm) grown atop 300 nm of SiO_2 on Si, b) XRD pattern of an In_2O_3 film grown on a quartz substrate.

Experimental Section

All experimental details (syntheses, ALD procedures, and characterization) are described in the Supporting Information.
CCDC 1819892 contains the supplementary crystallographic data for this paper. These data are provided free of charge by The Cambridge Crystallographic Data Centref.

Acknowledgements

This research was supported in part by the Center for the Next Generation of Materials by Design, an Energy Frontier Research Center funded by the U.S. DOE, Office of Science. This study was performed in part at the Center for Nanoscale Systems (CNS) at Harvard University, a member of the National Nanotechnology Infrastructure Network (NNIN), which is supported

© 2018 Wiley-VCH Verlag GmbH & Co. KGaA, Weinheim

by the National Science Foundation under NSF award no. ECS-0335765. We are grateful to Prof. Tonio Buonassisi (MIT) for letting us use his Hall effect measurement instrument.

Conflict of interest

The authors declare no conflict of interest.

Keywords: amidinate · atomic layer deposition · indium · thin films · transparent conducting oxide

[1] a) J.-S. Seo, J.-H. Jeon, Y. H. Hwang, H. Park, M. Ryu, S.-H. K. Park, B.-S. Bae, *Sci. Rep.* **2013**, *3*, 2085; b) S. Jeong, Y.-G. Ha, J. Moon, A. Facchetti, T. J. Marks, *Adv. Mater.* **2010**, *22*, 1346–1350; c) C. Hönes, A. Fuchs, S. Zweigart, S. Siebentritt, *IEEE J. Photovolt.* **2016**, *6*, 319–325; d) C. Bugot, N. Schneider, D. Lincot, F. Donsanti, *Beilstein J. Nanotechnol.* **2013**, *4*, 750–757.
[2] a) K. Ellmer, *Nat. Photonics* **2012**, *6*, 809–817; b) T. Minami, *Semicond. Sci. Technol.* **2005**, *20*, S35–S44.
[3] A. Kumar, C. Zhou, *ACS Nano* **2010**, *4*, 11–14.
[4] C. Xirouchaki, G. Kiriakidis, T. F. Pedersen, H. Fritzsche, *J. Appl. Phys.* **1996**, *79*, 9349–9352.
[5] a) N. H. Kim, J. H. Myung, H. W. Kim, C. Lee, *Phys. Status Solidi A* **2005**, *202*, 108–112; b) J. Ni, H. Yan, A. Wang, Y. Yang, C. L. Stern, A. W. Metz, S. Jin, L. Wang, T. J. Marks, J. R. Ireland, C. R. Kannewurf, *J. Am. Chem. Soc.* **2005**, *127*, 5613–5624.
[6] a) J. A. Libera, J. N. Hryn, J. W. Elam, *Chem. Mater.* **2011**, *23*, 2150–2158; b) S. M. George, *Chem. Rev.* **2010**, *110*, 111–131.
[7] V. Miikkulainen, M. Leskelä, M. Ritala, R. L. Puurunen, *J. Appl. Phys.* **2013**, *113*, 021301.
[8] a) W. J. Maeng, D.-w. Choi, K.-B. Chung, W. Koh, G.-Y. Kim, S.-Y. Choi, J.-S. Park, *ACS Appl. Mater. Interfaces* **2014**, *6*, 17481–17488; b) J. W. Elam, A. B. F. Martinson, M. J. Pellin, J. T. Hupp, *Chem. Mater.* **2006**, *18*, 3571–3578; c) R. K. Ramachandran, J. Dendooven, H. Poelman, C. Detavernier, *J. Phys. Chem. C* **2015**, *119*, 11786–11791; d) M. Ritala, T. Asikainen, M. Leskelä, *Electrochem. Solid-State Lett.* **1998**, *1*, 156–157; e) T. Asikainen, M. Ritala, M. Leskelä, *J. Electrochem. Soc.* **1994**, *141*, 3210–3213; f) W. J. Maeng, D.-W. Choi, J. Park, J.-S. Park, *J. Alloys Compd.* **2015**, *649*, 216–221; g) D.-J. Lee, J.-Y. Kwon, J. I. Lee, K.-B. Kim, *J. Phys. Chem. C* **2011**, *115*, 15384–15389; h) M. Gebhard, M. Hellwig, H. Parala, K. Xu, M. Winter, A. Devi, *Dalton Trans.* **2014**, *43*, 937–940; i) O. Nilsen, R. Balasundaraprabhu, E. V. Monakhov, N. Muthukumarasamy, H. Fjellvåg, B. G. Svensson, *Thin Solid Films* **2009**, *517*, 6320–6322; j) W. J. Maeng, D.-W. Choi, J. Park, J.-S. Park, *Ceram. Int.* **2015**, *41*, 10782–10787; k) H. Y. Kim, E. A. Jung, G. Mun, R. E. Agbenyeke, B. K. Park, J.-S. Park, S. U. Son, D. J. Jeon, S.-H. K. Park, T.-M. Chung, J. H. Han, *ACS Appl. Mater. Interfaces* **2016**, *8*, 26924–26931.
[9] Y. S. Lee, J. Heo, M. T. Winkler, S. C. Siah, S. B. Kim, R. G. Gordon, T. Buonassisi, *J. Mater. Chem. A* **2013**, *1*, 15416–15422.
[10] O. M. El-Kadri, I. M. Szilágyi, J. M. Campbell, K. Arstila, L. Niinistö, C. H. Winter, *J. Am. Chem. Soc.* **2006**, *128*, 9638–9639.
[11] a) J. A. Caraveo-Frescas, P. K. Nayak, H. A. Al-Jawhari, D. B. Granato, U. Schwingenschlögl, H. N. Alshareef, *ACS Nano* **2013**, *7*, 5160–5167; b) J. Heo, A. S. Hock, R. G. Gordon, *Chem. Mater.* **2010**, *22*, 4964–4973.
[12] M. D. Groner, F. H. Fabreguette, J. W. Elam, S. M. George, *Chem. Mater.* **2004**, *16*, 639–645.
[13] S. B. Kim, C. Yang, T. Powers, L. M. Davis, X. Lou, R. G. Gordon, *Angew. Chem. Int. Ed.* **2016**, *55*, 10228–10233; *Angew. Chem.* **2016**, *128*, 10384–10389.
[14] a) R. F. McCarthy, M. S. Weimer, J. D. Emery, A. S. Hock, A. B. F. Martinson, *ACS Appl. Mater. Interfaces* **2014**, *6*, 12137–12145; b) M. Gebhard, M. Hellwig, A. Kroll, D. Rogalla, M. Winter, B. Mallick, A. Ludwig, M. Wiesing, A. D. Wieck, G. Grundmeier, A. Devi, *Dalton Trans.* **2017**, *46*, 10220–10231.
[15] B. S. Lim, A. Rahtu, J.-S. Park, R. G. Gordon, *Inorg. Chem.* **2003**, *42*, 7951–7958.
[16] a) J. D. Halliday, E. A. Symons, *Can. J. Chem.* **1978**, *56*, 1463–1469; b) S. Vincent, C. Mioskowski, L. Lebeau, *J. Org. Chem.* **1999**, *64*, 991–997.

Manuscript received: May 8, 2018
Version of record online: June 5, 2018

© 2018 Wiley-VCH Verlag GmbH & Co. KGaA, Weinheim